Enhancement of Escherichia coli RecA protein enzymatic function by dATP

ARTICLE *in* BIOCHEMISTRY · AUGUST 1989

Impact Factor: 3.02 · DOI: 10.1021/bi00440a025 · Source: PubMed

2 AUTHORS, INCLUDING:

Joseph P Menetski
Merck
28 PUBLICATIONS **1,632** CITATIONS

SEE PROFILE

Eisenberg, E., & Hill, T. L. (1985) *Science 227*, 999–1006.
Geeves, M. A., & Gutfreund, H. (1982) *Febs. Lett. 140*, 11–15.
Geeves, M. A., & Halsall, D. J. (1986) *Proc. R. Soc. London, B 229*, 85–95.
Geeves, M. A., & Jeffries, T. E. (1988) *Biochem. J. 256*, 41–46.
Geeves, M. A., Goody, R. S., & Gutfreund, H. (1984) *J. Muscle Res. Cell Motil. 5*, 351–356.
Geeves, M. A., Jeffries, T. E., & Millar, N. C. (1986) *Biochemistry 25*, 8454–8458.
Goody, R. S., Hofmann, W., & Mannherz, H. G. (1977) *Eur. J. Biochem. 78*, 317–324.
Greene, L. E., & Eisenberg, E. (1980) *J. Biol. Chem. 255*, 543–548.
Hibberd, M. G., & Trentham, D. R. (1986) *Annu. Rev. Biophys. Chem. 15*, 119–161.
Hibberd, M. G., Dantzig, J. A., Trentham, D. R., & Goldman, Y. E. (1985) *Science 228*, 1317–1319.
Lehrer, S. S., & Kerwar, G. (1972) *Biochemistry 11*, 1211–1217.
Marston, S. B. (1982) *Biochem. J. 203*, 453–460.
Rosenfeld, S. S., & Taylor, E. W. (1984) *J. Biol. Chem. 259*, 11920–11929.
Rosenfeld, S. S., & Taylor, E. W. (1987) *J. Biol. Chem. 262*, 9984–9993.
Shriver, J. W., & Sykes, B. D. (1981) *Biochemistry 20*, 2004–2012.
Siemankowski, R. F., & White, H. D. (1984) *J. Biol. Chem. 259*, 5045–5053.
Siemankowski, R. F., Wiseman, M. O., & White, H. D. (1985) *Proc. Natl. Acad. Sci. U.S.A. 82*, 658–662.
Sleep, J. A., & Hutton, R. L. (1980) *Biochemistry 19*, 1276–1283.
Smith, S. J., & White, H. D. (1985) *J. Biol. Chem. 260*, 15156–15162.
Trentham, D. R., Bagshaw, C. R., & Eccleston, J. E. (1976) *Q. Rev. Biophys. 9*, 217–281.
Trybus, K. M., & Taylor, E. W. (1980) *Proc. Natl. Acad. Sci. U.S.A. 77*, 7209–7213.
Trybus, K. M., & Taylor, E. W. (1982) *Biochemistry 21*, 1284–1294.
Weeds, A. G., & Taylor, R. S. (1975) *Nature 257*, 54–57.
White, H. D. (1977) *Biophys. J. 17*, 40a.

Enhancement of *Escherichia coli* RecA Protein Enzymatic Function by dATP†

Joseph P. Menetski‡ and Stephen C. Kowalczykowski*
Department of Molecular Biology, Northwestern University Medical School, Chicago, Illinois 60611
Received November 29, 1988; Revised Manuscript Received March 22, 1989

ABSTRACT: The *Escherichia coli* recA protein has been shown to hydrolyze several nucleoside triphosphates in the presence of ssDNA. The substitution of dATP for rATP has significant effects on various recA protein biochemical properties. In the presence of dATP, recA protein can invade more secondary structure in native ssDNA than it can in the presence of rATP. The dATP–recA protein complex can compete more effectively with the *E. coli* ssDNA binding protein (SSB) for ssDNA binding sites compared with the rATP–recA protein complex. Finally, the rate of dATP hydrolysis stimulated by dsDNA is greater than the rate of rATP hydrolysis. These effects, in turn, are observed as alterations in the recA protein catalyzed DNA strand exchange reaction. In the absence of SSB protein, the rate of joint molecule and product formation in the DNA strand exchange reaction is greater in the presence of dATP than in the presence of rATP. The rate of product formation in the dATP-dependent reaction is also faster than the rATP-dependent reaction when SSB protein is added to the ssDNA before recA protein; the rate of rATP-dependent product formation is inhibited 10-fold under these conditions. This nucleotide, dATP, was previously shown to induce an apparent affinity of recA protein for ssDNA which is higher than any other NTP. These results suggest that the observed enhancement of enzymatic activity may be related to the steady-state properties of the high-affinity ssDNA binding state of recA protein. In addition, the data suggest that recA protein functions in NTP hydrolysis as a dimer of protein filaments and that the binding of ssDNA to only one of the recA filaments is sufficient to activate all recA protein molecules in the dimeric filament. The implications of this finding to the enzymatic function of recA protein are discussed.

RecA protein can catalyze the complete exchange of one single-stranded DNA (ssDNA)[1] molecule for a homologous strand within a duplex DNA molecule in a reaction called DNA strand exchange (Cox & Lehman, 1981a). This reaction requires the hydrolysis of a nucleoside triphosphate cofactor, typically rATP (Cox & Lehman, 1981a); however, the actual mechanistic requirement for rATP hydrolysis is unknown. Hypotheses for the role of rATP binding and hydrolysis in recA protein function include mediating the polar polymerization of recA protein on DNA (Griffith et al., 1984; Kowalczykowski et al., 1987), providing energy for concerted rotation of a recA protein filament to drive branch migration of heteroduplex joints (Schutte & Cox, 1987), and a way to

† This research was funded by a grant from the National Institutes of Health (AI-18987).
* Author to whom correspondence should be addressed.
‡ Present address: Laboratory of Molecular Biology, National Institutes of Health, Bethesda, MD.

[1] Abbreviations: PEP, phosphoenolpyruvate; ssDNA, single-stranded DNA; dsDNA, double-stranded DNA; etheno M13 DNA, modified M13 ssDNA containing 1,N^6-ethenoadenosine and 3,N^4-ethenocytidine residues; poly(dT), poly(thymidylic acid); poly(dA), poly(deoxyadenylic acid); poly(dA-dT), alternating copolymer of deoxyadenylic and thymidylic acid.

0006-2960/89/0428-5871$01.50/0

switch between high and low ssDNA affinity states, allowing recA protein to cycle on and off the DNA (Menetski & Kowalczykowski, 1985, 1987b). Studying the effects of nucleotides other than rATP on recA protein activities could further our understanding of the nucleotide hydrolysis requirement during DNA strand exchange.

Several nucleotides bind to (Weinstock et al., 1981; Kowalczykowski, 1986) and are hydrolyzed by (Weinstock et al., 1981; Menetski et al., 1988) recA protein. These nucleotides influence the affinity of recA protein for ssDNA (Menetski et al., 1988). The cofactor dATP induces the *highest* ssDNA affinity of all nucleoside triphosphates. Interestingly, the product of dATP hydrolysis, dADP, decreases the affinity of recA protein for ssDNA *less* than any other nucleoside diphosphate (Menetski et al., 1988). The rate of dATP hydrolysis by recA protein is faster than that of any other nucleoside triphosphate (Weinstock et al., 1981; Menetski et al., 1988). Also, dATP induces the most rapid rate of λ repressor proteolysis (Phizicky & Roberts, 1981; Resnick & Sussman, 1982; Cohen et al., 1983). Finally, dATP supports the formation of joint molecules by *Escherichia coli* recA protein (Weinstock, 1982) and is essential for catalysis of DNA strand transfer by a recA protein analogue from *Bacillus subtilis* (Lovett & Roberts, 1985). These properties of the dATP–recA protein complex led us to analyze further the effects of this nucleotide on recA protein enzymatic activities.

In this report, we show that the dATP–recA protein complex is a more capable competitor for ssDNA binding sites than the rATP–recA protein complex, as suggested by the result that dATP induces a very high affinity ssDNA binding state. Single-stranded DNA in regions of secondary structure that is not accessible to the rATP–recA protein complex stimulates dATP hydrolysis. In addition, the dATP–recA protein complex displaces SSB protein from ssDNA faster than the rATP–recA protein complex, and dATP hydrolysis is less inhibited by SSB protein under conditions that totally inhibit rATP hydrolysis. Finally, we show that the catalysis of the DNA strand exchange reaction is more proficient under conditions which are suboptimal for the rATP-stimulated reaction, when dATP is substituted for rATP. These results suggest that the enhanced binding properties of the dATP–recA protein complex are responsible for improving the enzymatic activities of recA protein.

Materials and Methods

Chemicals. All chemicals used were reagent grade, and solutions were made in glass-distilled H_2O. rATP was purchased from Boehringer Mannheim, and dATP was purchased from Sigma Chemical Co.; both were dissolved as concentrated stock solutions at pH 7.5. Concentrations of adenine nucleotides were determined spectrophotometrically by using an extinction coefficient of 1.54×10^4 cm^{-1} M^{-1} at 260 nm.

Proteins. RecA protein was purified from *E. coli* strain JC12772 (Uhlin & Clark, 1981) by using a preparative protocol (Kowalczykowski et al., unpublished observations) based on spermidine precipitation (Griffith & Shores, 1985). RecA protein concentration was determined by using an extinction coefficient of 2.7×10^4 cm^{-1} M^{-1} at 280 nm.

SSB protein was purified from strain RLM 727 by using a preparative protocol provided by Dr. Roger McMacken of The Johns Hopkins University. The concentration of SSB protein was determined by using an extinction coefficient at 280 nm of 3×10^4 cm^{-1} M^{-1}.

DNA. Phage M13 ssDNA and replicative form dsDNA were isolated as described by Messing (1983). The replicative form was linearized with *Eco*RI restriction endonuclease. The plasmid pBEU14 is nonhomologous to the M13 DNA and was prepared from strain BEU293 (kindly provided by A. John Clark of University of California at Berkley); pBEU is plasmid pBEU2 (Uhlin et al., 1983) containing the cloned *recA56* gene. The concentrations of ssDNA and dsDNA were determined by using extinction coefficients at 260 nm of 8784 and 6500 cm^{-1} M^{-1}, respectively.

Poly(dA), poly(dT), and poly(dA-dT) were purchased from P-L Biochemicals and dissolved in TE (10 mM Tris-HCl, pH 7.5, and 0.1 mM EDTA). The concentrations of the stock solutions were determined spectrophotometrically, and the extinction coefficients used were as follows: poly(dA), 8600 cm^{-1} M^{-1} at 259 nm; poly(dT), 8540 cm^{-1} M^{-1} at 257 nm; poly(dA-dT), 6800 cm^{-1} M^{-1} at 260 nm.

Etheno M13 DNA was made as described by Menetski and Kowalczykowski (1985). The concentration of this DNA was determined by using an extinction coefficient of 7.0×10^3 cm^{-1} M^{-1} at 260 nm (Menetski & Kowalczykowski, 1987a).

NTP Hydrolysis Assay. The rate of rATP and dATP hydrolysis was determined by using a enzyme-coupled spectrophotometric assay described previously (Kowalczykowski & Krupp, 1987). Typical buffer conditions consisted of 20 mM Tris-HCl (pH 7.5), 10 mM $MgCl_2$, and 0.1 mM dithiothreitol at 37 °C. The assay also contained 50 units/mL pyruvate kinase, 25 units/mL lactate dehydrogenase, and 1.5 mM PEP. It was determined that efficient regeneration of dATP required a higher concentration of pyruvate kinase than normally used for rATP regeneration (data not shown). Changes in these conditions are cited in the figure legends.

The apparent stoichiometry of recA protein binding to ssDNA can be determined from NTP hydrolysis assays. The concentration of recA protein required to saturate a given polynucleotide was determined by drawing a line through the initial linear region of the recA protein concentration dependence data and determining the point at which this line intercepts a line drawn through the end point of the curve parallel to the x axis. If the final data points were still increasing slightly, this line was estimated as a horizontal line to which the data were asymptotically approaching. The maximum rate of hydrolysis for a single recA protein monomer was determined by dividing the maximum rate of hydrolysis observed by the concentration of DNA-bound recA protein (as determined from the apparent DNA binding stoichiometry; above) to obtain the pseudo-first-order rate constant k_{cat}.

Experiments in the presence of SSB protein were carried out using either of two different experimental protocols. Normally, SSB protein was added to the reaction mixture after the recA protein–ssDNA complex had attained a steady-state rate of NTP hydrolysis. In an alternative experiment, called the "SSB protein displacement" reaction, SSB protein was added to the ssDNA before recA protein. The displacement reaction was initiated by the addition of recA protein and is characterized by a lag before the onset of steady-state nucleotide hydrolysis. The length of the lag phase has been determined by drawing a line through the final steady-state rate of hydrolysis and a line through the initial data points, parallel to the x axis. The intercept of these lines is reported as the length of the lag phase.

Coaggregation Assay. Coaggregation of M13 ssDNA and double-stranded pBEU14 DNA was conducted as described by Tsang et al. (1985) as modified below. Reactions were carried out in buffer containing 25 mM Tris–acetate (pH 7.5), 1 mM dithiothreitol, 1 mM NTP, and an NTP regenerating system (2.3 mM PEP and 50 units/mL pyruvate kinase). For reactions carried out in the presence of SSB protein (0.28 μM),

recA protein (2 μM) was first added to the M13 ssDNA (2.8 μM) in the presence of either rATP or dATP and 10 mM magnesium acetate. SSB protein was then added to the recA–ssDNA complex followed by the addition of pBEU14 dsDNA (10 μM). The reaction mixture was incubated at 37 °C for 10 min and then subjected to centrifugation in an Eppendorf centrifuge for 5 min. The amount of DNA in both the supernatant solution and the pellet was assessed by agarose gel electrophoresis. If coaggregation of the M13 ssDNA and the pBEU dsDNA by recA protein occurred, both DNA molecules were found in the pellet. For reactions carried out in the absence of SSB protein, the recA protein–ssDNA complex was incubated in buffer containing 1 mM magnesium acetate and either rATP or dATP. Double-stranded DNA and magnesium acetate (10 mM final concentration) were then added to the reaction simultaneously. The reaction mixture was treated as described above to determine the amount of coaggregation.

DNA Strand Exchange Assay. The agarose gel assay for measuring DNA strand exchange was conducted as described previously (Cox & Lehman, 1981b; Roman & Kowalczykowski, 1986). However, in this paper, DNA samples were subjected to electrophoresis on 0.8% agarose gels in the absence of ethidium bromide and later stained to visualize the DNA bands. This procedure allows separation of the product of the DNA strand exchange reaction, gapped circular duplex DNA, from intermediate species (Menetski, 1988). Intermediates in this reaction are plectonemic joint molecules containing both strands of the dsDNA molecule and the invading ssDNA molecule (Cox & Lehman, 1981a; Menetski, 1988). Reactions are typically run in buffer containing 25 mM Tris–acetate (pH 7.5), 1 mM dithiothreitol, 8 mM $Mg(OAc)_2$, and 1 mM nucleotide triphosphate at 37 °C. The concentrations of M13 ssDNA and linear dsDNA were 10 and 20 μM, respectively, unless indicated. The concentration of recA protein was 6 μM, and SSB protein, when included, was present at 0.9 μM. An rATP and dATP regenerating system, containing 25 units/mL pyruvate kinase and 7.5 mM PEP, was included in all of the reactions. The stained gels were photographed by using Polaroid type 55 positive/negative film, and the negative was scanned by using a Zenieh soft laser scanning densitometer. The percent of product and intermediate was determined as the percent of DNA in the product (gapped duplex) or in all of the intermediates (joint molecules) divided by the total DNA (linear duplex substrate + gapped duplex product + intermediate species).

Results

RecA Protein Can Use ssDNA Possessing Secondary Structure for Nucleotide Hydrolysis More Effectively in the Presence of dATP than rATP. RecA protein cannot utilize all of the M13 ssDNA molecule as a substrate for rATPase activity due to limitations imposed by the presence of secondary structure (Muniyappa et al., 1984; Tsang et al., 1985; Kowalczykowski & Krupp, 1987). Since the dATP–recA protein complex shows a higher affinity for ssDNA compared to all other NTP–recA protein complexes, the dATPase activity may not be limited by secondary structure in the ssDNA. To test this, the amount of M13 ssDNA available to recA protein as a substrate for dATP hydrolysis was determined both in the absence and in the presence of SSB protein by examining the recA protein concentration dependence of NTP hydrolysis.

At a constant ssDNA concentration, the rate of NTP hydrolysis increases with increasing protein concentration until the available DNA is fully saturated and then becomes independent of protein concentration (Figure 1). In the absence of SSB protein and the presence of rATP, apparent saturation of the DNA occurs at 0.54 μM recA protein, yielding an apparent site size for recA protein of approximately 5.6 nucleotides per recA protein monomer (Table I). In the presence of SSB and rATP, the observed site size is approximately 2.7 nucleotides/recA protein monomer. These values differ from those reported previously (Kowalczykowski & Krupp, 1987) due to differences in the method used to determine the point at which saturation occurred. The data suggest that, in the absence of SSB protein, the M13 ssDNA contains secondary structure that does not support rATP hydrolysis. The addition of SSB protein disrupts this secondary structure, such that these regions of DNA can be used by recA protein to stimulate rATP hydrolysis (Kowalczykowski & Krupp, 1987). Thus, the addition of SSB protein increases the concentration of recA protein required to saturate the DNA.

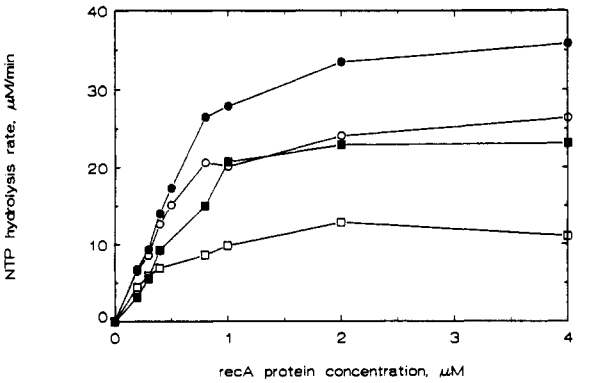

FIGURE 1: Effect of recA protein concentration on the M13 ssDNA dependent hydrolysis of rATP and dATP. Reactions were conducted using standard NTP hydrolysis conditions (see Materials and Methods). The concentration of nucleotide was 500 μM, M13 ssDNA was 3 μM, and SSB protein, when added, was 0.6 μM. The symbols represent rATP hydrolysis without SSB protein (open squares), rATP hydrolysis with SSB protein (closed squares), dATP hydrolysis without SSB protein (open circles), and dATP hydrolysis with SSB protein (closed circles).

Table I: Comparison of the RecA Protein rATPase and dATPase Activities Stimulated by Various DNA Substrates

DNA	SSB	NTP	app site size[a] (nucleotides)	max rate of hydrolysis[b] (μM NTP min^{-1})	k_{cat}[c] (min^{-1})
ssM13	−	rATP	5.6	12	22
ssM13	+	rATP	2.7	23	21
ssM13	−	dATP	3.4	26	29
ssM13	+	dATP	2.8	36	33
poly(dA)		rATP	6.3	9.6	21
poly(dA)		dATP	3.3	21	23
poly(dT)		rATP	3.1	24	26
poly(dT)		dATP	3.1	31	32
etheno M13		rATP	3.0	30	30
etheno M13		dATP	3.1	34	35
poly(dA-dT)		rATP	7.1	17	21
poly(dA-dT)		dATP	5.6	22	21

[a] Experiments were done as described under Materials and Methods. The concentration of ssDNA used was 3 μM; 500 μM either rATP or dATP and 0.6 μM SSB protein, when used. The concentration of poly(dA-dT) was 6 μM nucleotides. The apparent site size for each complex was determined as described under Materials and Methods. The value is reported as nucleotide residues of DNA per recA protein monomer. These values are reproducible within ±0.5 nucleotide residue per recA protein monomer. [b] The maximum rate of hydrolysis is reported as micromolar NTP hydrolyzed per minute at the highest protein concentration tested. The error on these rate determinations is within 5% of the given average. [c] k_{cat} values were determined as described under Materials and Methods and are reported as min^{-1}. These values are reproducible within 10% of the given average.

When dATP is substituted for rATP, the apparent site size in the absence of SSB protein is decreased (Figure 1; Table I). This suggests that in the absence of SSB protein, the dATP–recA protein complex can access more DNA within secondary structure than the rATP–recA protein complex. Addition of SSB protein results in a 20% decrease in the apparent site size (Figure 1; Table I), suggesting that there is still some secondary structure in the ssDNA which is unavailable to the dATP–recA protein complex.

The observed rate of nucleotide hydrolysis at saturating protein concentrations is different for each complex and is greater for each in the presence of SSB protein (Figure 1). However, these apparent differences could be the result of variations in the amount of recA protein bound to ssDNA. The maximum rate of hydrolysis for each active recA protein monomer (k_{cat} or turnover number) was determined by dividing the hydrolysis rate observed at saturation by the concentration of recA protein required to saturate the DNA. This procedure gives the maximum number of nucleotides hydrolyzed per recA monomer per minute. As shown in Table I, the value of k_{cat} for rATP hydrolysis is the same in the absence and presence of SSB protein. This result is also found for dATP hydrolysis; k_{cat} values for dATP hydrolysis are 30 (±1.5) and 33 (±1.7) dATP molecules per minute per recA molecule in either the absence or the presence of SSB, respectively. Since the turnover of either rATP or dATP by recA protein is not changed by the presence of SSB protein, these data suggest that SSB protein is not influencing the catalytic rate of NTP hydrolysis. It is more likely that SSB protein is just increasing the amount of active recA protein formed (i.e., recA protein bound to ssDNA).

Properties of Polynucleotide-Dependent NTP Hydrolysis. The analysis of the NTPase activity data using M13 ssDNA as a substrate is complicated by the presence of an unknown amount of secondary structure. Therefore, the protein concentration dependence of NTP hydrolysis was examined by using various polynucleotides lacking secondary structure. We used two homopolymers, poly(dA) and poly(dT), and etheno M13 DNA which has been modified at all adenine and cytosine bases (Menetski & Kowalczykowski, 1985; Menetski et al., 1988). As determined from nucleotide hydrolysis, the apparent site size of recA protein is approximately the same for poly(dT) and etheno M13 DNA in the presence of either rATP or dATP (Table I). In the presence of dATP, the apparent site size of recA protein for poly(dA) is also similar to that of poly(dT) and etheno M13 DNA (Table I). Interestingly, in the presence of rATP, the site size of recA protein for poly(dA) is twice that observed in the presence of dATP. With this exception, the hydrolytically active recA protein has an apparent site size of approximately 3. This is the same site size observed for M13 ssDNA in the presence of SSB protein.

The turnover number (k_{cat}) for each polynucleotide was determined and is also shown in Table I. The rATP hydrolysis rates are in good agreement with those previously published (Kowalczykowski & Krupp, 1987; Menetski et al., 1988). Thus, although the apparent site size of recA protein for poly(dA) is twice that expected in the presence of rATP, the turnover number of the bound (active) recA protein is unchanged. These data suggest that less recA protein is stimulated for NTP hydrolysis by poly(dA) in the presence of rATP than in the presence of dATP.

Stimulation of dATP Hydrolysis by SSB Protein Is Dependent on dATP Concentration. The stimulation of rATP hydrolysis by SSB protein is dependent on rATP concentration (Kowalczykowski & Krupp, 1987). At low rATP concentrations (<150–200 μM), SSB protein inhibits rATP hydrolysis; as rATP concentration is increased, SSB protein stimulates the rate of rATP hydrolysis. The dATP concentration dependence of hydrolysis in the absence and presence of SSB protein is shown in Figure 2. Below 70 μM dATP, SSB protein inhibits dATP hydrolysis, whereas above this concentration SSB protein stimulates dATP hydrolysis.

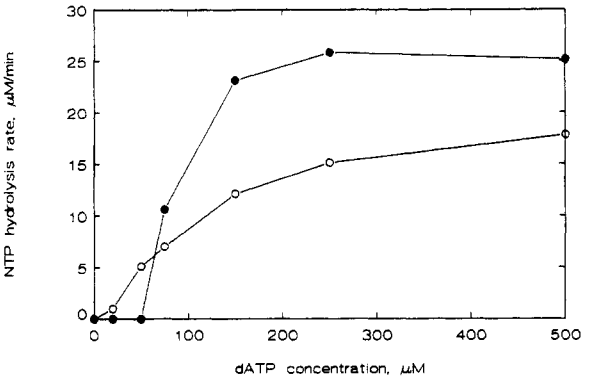

FIGURE 2: Effect of dATP concentration on nucleotide hydrolysis. Reactions were conducted using standard NTP hydrolysis conditions (see Materials and Methods). The concentrations of M13 ssDNA and recA protein were 3 and 0.8 μM, respectively. SSB protein concentration, when added, was 0.6 μM. The symbols represent the rate of dATP hydrolysis without SSB protein (open circles) and with SSB protein (closed circles).

Stimulation of dATP Hydrolysis by SSB Protein Is Not Dependent on Magnesium Ion Concentration. The hydrolysis of rATP is inhibited by SSB protein at low (1–2 mM) magnesium chloride concentrations (Roman & Kowalczykowski, 1986; Kowalczykowski & Krupp, 1987). For comparison, the magnesium chloride concentration dependence of dATP hydrolysis was determined. In the absence of SSB protein, the rate of dATP hydrolysis using M13 ssDNA as a substrate is essentially constant from 1 to 15 mM magnesium chloride (not shown). In contrast to rATP hydrolysis, dATP hydrolysis is not inhibited and is actually stimulated by SSB protein at all magnesium concentrations tested. Therefore, the dATP–recA protein complex competes more effectively than the rATP–recA protein complex with SSB protein for limiting ssDNA binding sites at lower magnesium ion concentrations.

Displacement of SSB Protein from ssDNA Is Stimulated by dATP. The formation of an SSB protein–ssDNA complex before the addition of recA protein inhibits the rate of rATP hydrolysis by recA protein (Kowalczykowski & Krupp, 1987; Lavery & Kowalczykowski, 1988). In a slow, time-dependent reaction, the rATP–recA protein complex displaces some SSB protein from the ssDNA and establishes a steady-state rate of rATP hydrolysis. During the initial displacement of SSB protein, very little rATP hydrolysis occurs. Thus, the rate of SSB displacement by recA protein is inversely proportional to the length of the lag time prior to the onset of steady-state nucleotide hydrolysis. In the presence of 1 mM rATP, there is a lag in steady-state rATP hydrolysis for approximately 870 s, followed by a steady-state rate of rATP hydrolysis of 14 μM rATP/min (Table II). This hydrolysis rate is about 60% of that observed when SSB protein is added after recA protein. In the presence of 1 mM dATP, the lag in dATP hydrolysis is only 300 s followed by a final rate of dATP hydrolysis of 32 μM dATP/min. This rate of dATP hydrolysis is similar to that when SSB protein is added after recA protein. The data show that the dATP–recA protein complex displaces SSB protein from ssDNA faster than the rATP–recA protein complex and establishes a faster final steady-state rate of NTP hydrolysis.

Table II: Effect of Nucleotide Concentration on SSB Displacement by RecA Protein

[nucleotide]	lag (s)[a]	steady-state rate (μM NTP/min)
1 mM dATP	300	32
1 mM rATP	870	14
500 μM rATP	880	13
250 μM rATP	1390	8.5
100 μM rATP	1990	0.27

[a] Experiments were conducted as described under Materials and Methods. Lags and steady-state rates were evaluated as described under Materials and Methods. The component concentrations were 3 μM M13 ssDNA, 1 μM recA protein, and 0.6 μM SSB protein in standard rATPase assay buffer at 37 °C.

In the cell, there is an excess of rATP over dATP (3 mM rATP and 175 μM dATP; Bochner & Ames, 1982). To determine whether low concentrations of dATP could stimulate SSB protein displacement in the presence of high concentrations of rATP, the dATP concentration dependence of SSB protein displacement has been determined at several fixed rATP concentrations. Increasing the dATP concentration in the presence of rATP could have two separate effects on SSB displacement: (1) dATP could decrease the lag in nucleotide hydrolysis; (2) it could increase the final steady-state rate of NTP hydrolysis. To simplify quantification of the stimulatory effect of dATP on SSB displacement, the data have been transformed to show only the enhancement by dATP. Stimulation of the lag phase of NTP hydrolysis (S_L) represents the decrease in the lag by the addition of dATP [lag(without dATP) − lag(with dATP)]. Similarly, dATP stimulation of the rate (S_R) is presented as the increase in the steady-state rate of hydrolysis by the addition of dATP.

As dATP concentration is increased, the lag phase of the reaction decreases at each fixed, rATP concentration (Figure 3A; i.e., S_L increases). The amount that the lag is decreased by dATP, at high dATP concentration, decreases with increasing fixed rATP concentration. A similar pattern of stimulation is observed for the rate data (Figure 3B). The decrease in plateau value, of both S_L and S_R, is due to a decrease in the lag phase (and increase in the rate) observed when rATP concentration is increased in the absence of dATP (see Table II for ATP alone and dATP alone data). The important point is that dATP still stimulates the rate of SSB displacement (reduces the lag) and increases the steady-state rate of hydrolysis at all rATP concentrations tested. At high dATP concentrations, in these experiments, the stimulation by dATP is enough to show displacement properties similar to those observed with dATP alone (i.e., lag = 300 s, rate = 28 μM NTP/min). This is true even when both the lag phase and the steady-state rate show saturation with rATP alone (i.e., above 500 μM, Table II). These data demonstrate that at all rATP concentrations, dATP can stimulate the SSB protein displacement reaction and that in a mixture of rATP and dATP and NTP–recA protein complex can have the properties of the dATP(alone)–recA protein complex (see Table II).

The apparent K_m for dATP at each rATP concentration was determined by fitting each data set to a hyperbola. Computed curves are shown on Figure 3. The apparent K_m values from each set of curves (lag and steady-state rate) were then plotted versus rATP concentration (Figure 4). The data show that the apparent K_m values for dATP in the presence of rATP increase with rATP concentration and seem to saturate at high rATP concentrations. The resultant data have also been fit to a hyperbola to determine the maximum apparent K_m for dATP (i.e., the maximum of the hyperbolic fit). The data show that the maximum apparent K_m for dATP determined from the lag data is approximately 160 μM dATP, while that determined from the rate data is approximately 400 μM.

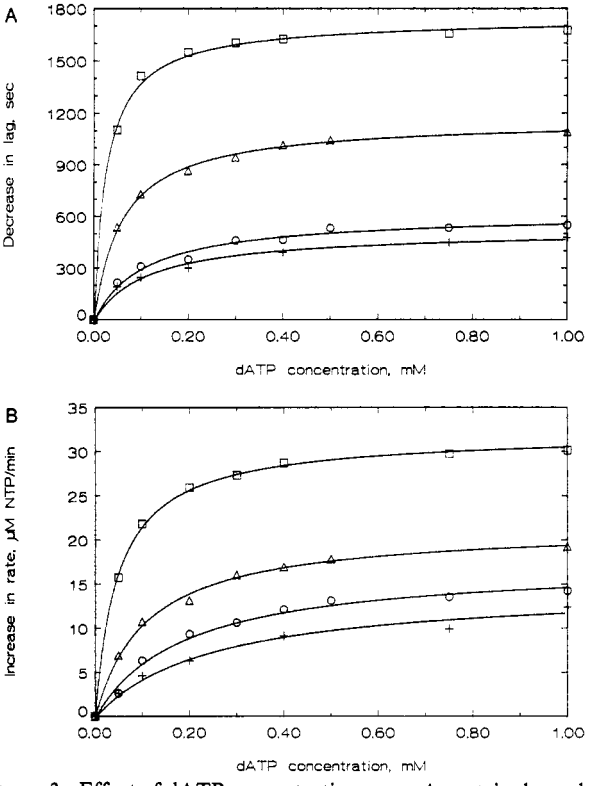

FIGURE 3: Effect of dATP concentration on recA protein dependent displacement of SSB protein from ssDNA. Experiments were done in standard nucleotide hydrolysis buffer containing added rATP and dATP at the concentrations shown. Reactions were started by adding 1 μM recA protein to a complex of 0.6 μM SSB protein and 3 μM M13 ssDNA. (A) Effect of dATP concentration on the lag in nucleotide hydrolysis. (B) Effect of dATP concentration on the rate of nucleotide hydrolysis. 100 μM rATP (squares); 250 μM rATP (triangles); 500 μM rATP (circles); 1 mM rATP (crosses).

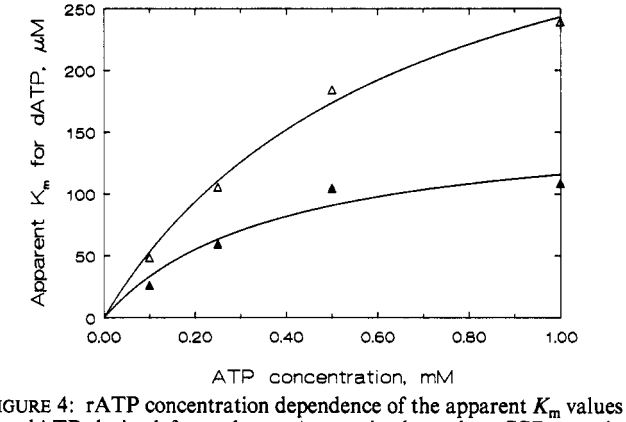

FIGURE 4: rATP concentration dependence of the apparent K_m values for dATP derived from the recA protein dependent SSB protein displacement reaction. Each data set from Figure 3 was fit to a hyperbola, and the half-maximal dATP concentration (the apparent K_m for dATP) obtained from the lag data (closed triangles) and rate data (open triangles) is plotted as a function of rATP concentration. These data were then fit to a hyperbola. The maximum apparent K_m values for dATP determined in this way are 160 and 405 μM for the lag and rate data, respectively. The half-maximum rATP concentrations determined from these data are 381 and 665 μM for the lag and rate data, respectively.

dATPase Activity of RecA Protein Stimulated by Etheno M13 ssDNA Shows Greater Resistance to Inhibition by SSB Protein. SSB protein inhibits ssDNA-dependent rATPase activity of recA protein when polynucleotides which cannot form secondary structure are used (Kowalczykowski & Krupp, 1987). This inhibitory effect of SSB protein was examined

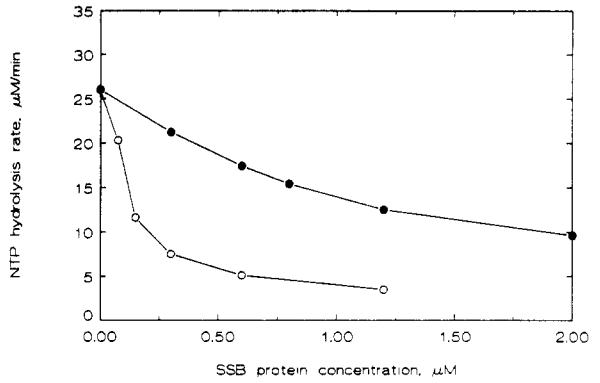

FIGURE 5: Inhibition of etheno M13 DNA dependent dATP hydrolysis by SSB protein. Reactions were conducted using standard hydrolysis conditions (see Materials and Methods). The concentration of nucleotide was 500 μM. The concentration of etheno M13 DNA was 3 μM, and the concentration of recA protein was 0.8 μM. SSB protein was added, at the concentration indicated, to the reaction mixture containing DNA either before recA protein (open circles) or after recA protein (closed circles).

for dATP hydrolysis using etheno M13 DNA as the polynucleotide cofactor. When SSB protein was added to etheno M13 DNA prior to the addition of recA protein, the rate of dATP hydrolysis was inhibited stoichiometrically with increasing SSB protein concentration (Figure 5). An apparent monomer site size for SSB protein of approximately 15 nucleotides/protein monomer can be determined from these data. This value is in good agreement with published data (Bujalowski & Lohman, 1986; Kowalczykowski & Krupp, 1987). In contrast to the results in the presence of rATP (Kowalczykowski & Krupp, 1987), dATP hydrolysis is not completely inhibited, even at high SSB concentrations (>0.6 μM SSB).

The rate of etheno M13 DNA dependent rATP hydrolysis is inhibited by SSB protein regardless of the order of addition (Kowalczykowski & Krupp, 1987). When SSB protein is added last to a reaction, the rate of rATP hydrolysis decreases with time to an apparent steady-state rate which is equal to that observed when SSB protein is added to the DNA before the addition of recA protein. A time-dependent decrease in the rate of nucleotide hydrolysis is also observed in the presence of dATP, although it is slower than for rATP (not shown). However, unlike rATP hydrolysis, the final observed rate of dATP hydrolysis is different depending on whether SSB protein is added before or after recA protein (Figure 5). Compared to rATP hydrolysis, the rate of dATP hydrolysis is much less inhibited by the addition of SSB protein after recA protein. Addition of 0.4 μM SSB protein to a reaction mixture after recA protein inhibits dATPase activity by less than 30% (Figure 5), whereas this concentration of SSB protein completely inhibits rATP hydrolysis (Kowalczykowski & Krupp, 1987). Therefore, these results also suggest that the dATP–recA protein complex can compete with SSB protein for ssDNA binding sites better than the rATP–recA protein complex.

Rate of dsDNA-Dependent Nucleotide Hydrolysis Is Greater for dATP than for rATP. Double-stranded DNA can stimulate rATP hydrolysis by recA protein (Roman & Kowalczykowski, 1986; Kowalczykowski et al., 1987; Pugh & Cox, 1987). The time course of the dsDNA-dependent hydrolysis reaction is characterized by a long lag, thought to be involved in a DNA "opening" step, followed by an apparent steady-state rate of hydrolysis (Kowalczykowski et al., 1987). A comparison of the lag and steady-state rates of both rATP and dATP hydrolysis stimulated by linear M13 dsDNA is presented in Table III. The lag time in dATP hydrolysis is only

Table III: Properties of M13 dsDNA Dependent Hydrolysis of rATP and dATP[a]

nucleotide	lag (s)[b]	rate of hydrolysis[c] (μM min^{-1})
rATP	980	8.9
dATP	200	22

[a] Nucleotide hydrolysis reactions were conducted in standard hydrolysis buffer. The constituent concentrations were 1 mM NTP, 6 μM M13 dsDNA, and 2.1 μM recA protein. [b] Lag times were determined by the intersection of a line through the final steady-state slope and a line parallel to the x axis and through the initial absorbance. [c] Final steady-state rates were determined from the linear region of nucleotide hydrolysis with time after the lag phase.

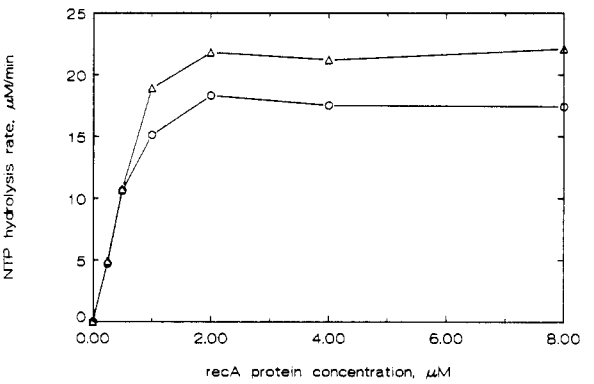

FIGURE 6: Effect of recA protein concentration on dsDNA-dependent rATP and dATP hydrolysis. Reactions were conducted using standard hydrolysis conditions (see Materials and Methods). The concentration of nucleotide was 500 μM, and poly(dA-dT) concentration was 6 μM nucleotide residues. The protein dependence was determined in the presence of rATP (circles) and dATP (triangles).

20% that observed for rATP, and the final steady-state rate of dATP hydrolysis is more than twice that of rATP.

The reduction of the lag phase suggests that the DNA opening step is much faster with dATP than with rATP. The difference in the apparent steady-state rate could be due to one of two possibilities: (1) the rate of dsDNA-dependent dATP hydrolysis (i.e., k_{cat}) is intrinsically faster than that for rATP; or (2) the steady-state amount of dATP–recA protein complex bound to dsDNA is greater than the equivalent rATP complex. To distinguish between these two possibilities, the recA protein concentration dependence of NTP hydrolysis was determined using poly(dA-dT) as the substrate. This substrate is more homogeneous than native M13 dsDNA and shows an easily definable lag phase. The lag phase observed when this substrate is used is shorter than when M13 dsDNA is used (190 ± 2 s with dATP and 240 ± 5 s with rATP, not shown). Figure 6 shows that as recA protein concentration is increased, the rate of hydrolysis of either rATP or dATP is increased. The concentrations of recA protein required to saturate the DNA in the presence of either rATP or dATP are similar; apparent site sizes of 7.1 (±0.2) and 5.6 (±0.1) nucleotides per recA protein monomer are observed in the presence of either rATP or dATP, respectively. The small difference in the apparent site sizes of the two complexes may suggest that more of the dsDNA is available to the dATP–recA protein complex to stimulate hydrolysis. The final plateau rate of dATP hydrolysis is greater than that of rATP hydrolysis, however, not by the 2-fold which is observed with native M13 dsDNA as a substrate. When corrected for differences in binding stoichiometries, the resultant k_{cat} values are identical (Table I).

RecA Protein Dependent Coaggregation of Single- and Double-Stranded DNA Occurs in the Presence of dATP.

Table IV: Rates of Intermediate and Product Formation in the DNA Strand Exchange Reaction[a]

SSB	NTP	intermediate formation (pM/min)	product formation (pM/min)
none[b]	rATP	4.0	0.3
none[b]	dATP	6.5	0.8
SSB second[b]	rATP	51	45
SSB second[b]	dATP	52	21
SSB first[c]	rATP		5.2
SSB first[c]	dATP		21
SSB second[c]	rATP		52
SSB second[c]	dATP		32

[a] The rates of intermediate and product formation were determined as described under Materials and Methods. Rates are reported as picomolar dsDNA molecules per minute. The error associated with each value is approximately 10%. [b] These rates were determined from reactions using 10 μM M13 dsDNA nucleotides (695 pM dsDNA molecules). SSB 2nd means that SSB protein was added to the reaction mixture 1 min after the addition of recA protein; none means that no SSB protein was included. [c] These rates were determined by using the data in Figure 7 in which 20 μM M13 dsDNA nucleotides (1.4 nM dsDNA molecules) was used. SSB 1st means that SSB protein was added to the reaction mixture 1 min before the addition of recA protein, while SSB 2nd means SSB protein was added 1 min after the addition of recA protein.

RecA protein can form high molecular weight aggregates of ssDNA and dsDNA, termed coaggregates, which have been suggested to be intermediates in the in vitro DNA strand exchange reaction (Tsang et al., 1985). Under conditions which allow the complete saturation of the ssDNA molecule (i.e., either in the presence of SSB protein or with preincubation in 1 mM magnesium ion), coaggregation can occur between any ssDNA and dsDNA molecule, even in the absence of homology (Tsang et al., 1985). We analyzed the coaggregation reaction in the presence of dATP and found that dATP is as effective at stimulating coaggregation as rATP. In the presence of SSB protein, greater than 95% of the single- and double-stranded DNA was found in these high molecular weight coaggregates in the presence of either rATP or dATP (not shown). Also, >95% of both the ssDNA and the dsDNA was found in the coaggregates after preincubation at 1 mM magnesium ion in the presence of either rATP or dATP. These data show that dATP, like rATP, can stimulate the formation of these intermediates in vitro.

dATP Can Stimulate the in Vitro DNA Strand Exchange Reaction. The DNA strand exchange reaction of recA protein requires the binding and hydrolysis of rATP (Cox & Lehman, 1981a). Since several properties of dATP hydrolysis differ significantly from those of rATP hydrolysis, the influence of dATP on this complex reaction was examined. Agarose gel electrophoresis in the absence of ethidium bromide can resolve plectonemic joint molecules (containing both circular M13 ssDNA and linear M13 dsDNA) from product gapped duplex molecules; this permits analysis of both the rate of stable joint molecule formation and the rate of product formation in a single assay (Menetski, 1988).

In the absence of SSB protein, less than 10% of the linear M13 dsDNA is converted to joint molecules in the rATP-dependent DNA strand exchange reaction (not shown). Also, only a small amount (<5%) of final product (gapped circular M13 dsDNA) is formed after 80 min. In contrast, almost 20% of the linear M13 dsDNA is converted to stable joint molecules in the presence of dATP. Coincident with an increase in the amount of joint molecules formed, a greater amount of product is formed (≈6% after 80 min) in the presence of dATP. The rates of joint molecule and product formation in the presence of either rATP or dATP under these conditions are shown in Table IV. The initial rate of joint molecule formation in the absence of SSB protein is approximately 1.5 times faster when dATP is substituted for rATP. Likewise, the maximum rate of product formation under these conditions is 2.5 times greater in the presence of dATP rather than rATP. Thus, in the absence of SSB protein, substitution of dATP for rATP enhances the ability of recA protein to catalyze the DNA strand exchange reaction.

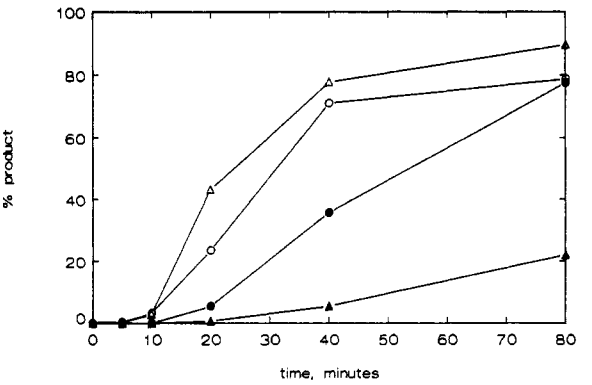

FIGURE 7: Effect of the order of SSB protein addition on the DNA strand exchange reaction. Reactions were done in standard DNA strand exchange assay conditions as described under Materials and Methods (10 μM M13 ssDNA and 20 μM M13 dsDNA). Final product formation in the presence of rATP when SSB was added first (closed triangles), rATP when SSB was added second (open triangles), dATP when SSB was added first (closed circles), and dATP when SSB was added second (open circles).

SSB protein stimulates the DNA strand exchange reaction when it is added to the recA protein–ssDNA complex (Cox & Lehman, 1981a). In the rATP-dependent reaction, approximately 80% of the linear M13 dsDNA is converted into joint molecules in 10 min (not shown). The amount of joint molecules then decreases with a concomitant increase in the amount of product-gapped M13 dsDNA molecules which is nearly complete after 20 min. In the presence of dATP, the time course of joint molecule formation is very similar to that of the rATP-dependent reaction, except the rate of decrease after 10 min is slower (Menetski, 1988). The increase in the amount of product formed in the presence of dATP is slower than that observed in the presence of rATP (Figure 7; Table IV).

The difference between rATP and dATP in the rate of final product formation, when SSB protein is added after recA protein, may be misleading. In the presence of dATP, by 10 min approximately 70–80% of the input DNA is converted into a species that hardly migrates into the gel. This species probably represents a DNA network molecule formed after repeated initiation events on a given dsDNA molecule (Chow et al., 1988). Reinitiation requires displacement of SSB protein from the newly displaced ssDNA strand, and we have demonstrated that, in the presence of dATP, recA protein can effectively displace SSB protein (Figure 3 and see below). These networks represent kinetically trapped intermediates since, with time, they are converted to product molecules. Under reaction conditions which inhibit the formation of this network species (e.g., 6 mM magnesium acetate and 3 mM PEP), the rates of intermediate and final product formation in the presence of either rATP or dATP are the same within error (Menetski and Kowalczykowski, unpublished observations).

Early studies on the in vitro DNA strand exchange reaction determined that there was a dependence on the order in which protein components were added to a reaction mixture (Cox & Lehman, 1982). Since the dATP–recA protein complex

can displace SSB protein from ssDNA better than the rATP complex, DNA strand exchange was examined when SSB protein is added to the ssDNA before recA protein. As shown in Figure 7, the rate of product formation in the presence of rATP is inhibited approximately 10-fold by reversing the order of addition of SSB protein and recA protein. The rates of product formation for Figure 7 are shown in Table IV. In the presence of dATP, the order of addition of recA and SSB protein has much less of an effect on product formation. This result suggests that the enhanced ability of the dATP–recA protein complex to displace SSB protein from ssDNA, as measured by the ssDNA-dependent NTP hydrolysis assay, moderates the order of addition constraint on the in vitro DNA strand exchange reaction.

Discussion

In this paper, we examined the effects of the nucleotide cofactor dATP on the enzymatic properties of the *E. coli* recA protein. This nucleotide induces a high-affinity ssDNA binding state of recA protein which has a greater stability than that induced by any other nucleoside triphosphate (Menetski et al., 1988). dATP has a marked effect on many properties of recA protein. Perhaps most significantly, the dATP-dependent DNA strand exchange reaction is enhanced under conditions which are not optimal for DNA strand exchange in the presence of rATP. In the absence of SSB protein or if SSB protein is added to the ssDNA first, dATP promotes the DNA strand exchange reaction more efficiently than rATP. In both cases, these enhanced properties of the dATP-dependent DNA strand exchange reaction are presumably related to the increased ability of the dATP–recA protein complex to compete for ssDNA binding sites. In the absence of SSB protein, the dATP–recA protein complex can disrupt more secondary structure in ssDNA than the rATP complex; in the presence of SSB protein, the dATP–recA protein complex can displace SSB protein from ssDNA more effectively than the rATP complex. The physical basis for these effects is likely due to the greater steady-state stability of the dATP–recA protein–ssDNA complex, which must result from an altered kinetic property (i.e., increased association or decreased dissociation rate).

The apparent site size of recA protein, determined by M13 ssDNA dependent rATP hydrolysis (Table I), is approximately 5.6 nucleotides per recA protein. When SSB protein is present, the apparent site size of recA protein for M13 ssDNA is approximately 3.2 nucleotides per recA protein; this value is similar to those observed using polynucleotides devoid of secondary structure. Thus, about twice as much recA protein is required to saturate either M13 ssDNA in the presence of SSB or ssDNA that does not contain any secondary structure. The observed rate of M13 ssDNA dependent rATP hydrolysis doubles upon the addition of SSB protein (Figure 1). Thus, the maximum rate of rATP hydrolysis per bound recA protein monomer (k_{cat}) is the same both in the presence and in the absence of SSB protein. These data are consistent with a hypothesis that recA protein cannot utilize some of the M13 ssDNA substrate in the absence of SSB protein, because it is sequestered in secondary structure which recA protein alone cannot disrupt (Kowalczykowski & Krupp, 1987). SSB protein removes the secondary structure in the DNA, and the liberated ssDNA can be used by recA protein to stimulate nucleotide hydrolysis. Morrical et al. (1986) reported that SSB protein increased the maximum rate of rATP hydrolysis per recA protein. However, the k_{cat} determined with M13 ssDNA (either in the absence or in the presence of SSB protein) compares very well with that observed by using polynucleotides that contain no secondary structure (in the absence of SSB). These data suggest that the active recA protein in each case is similar and that SSB protein affects only the amount of recA protein bound to the ssDNA.

In the presence of dATP, SSB protein has a smaller effect on the apparent site size of recA protein for ssDNA than in the presence of rATP. In the absence of SSB protein, the apparent site size of recA protein for polynucleotides not containing secondary structure is similar to that for M13 ssDNA. Therefore, in the presence of dATP, recA protein can disrupt secondary structure in M13 ssDNA which it cannot in the presence of rATP. Thus, one possible reason that the dATP–recA protein complex can catalyze DNA strand exchange better in the absence of SSB protein, than the rATP complex, may be that there is less inhibitory secondary structure remaining in the ssDNA. However, the rate and extent of DNA strand exchange are still less in the absence of SSB protein than in its presence. Since SSB protein still stimulates the rate of dATP hydrolysis by recA protein, there may be some secondary structure that even the dATP–recA protein complex cannot disrupt which inhibits DNA strand exchange.

Previous studies have suggested that the high-affinity ssDNA binding state of recA protein is important in the competition with SSB protein for ssDNA binding sites (Kowalczykowski & Krupp, 1987; Kowalczykowski et al., 1989). We have found that the dATP–recA protein complex can displace SSB protein from ssDNA more effectively than the rATP–recA protein complex (Figure 3). The length of the lag phase is much shorter in the presence of dATP than with rATP (300 versus 800 s, respectively), indicating that the rate of SSB protein displacement is more rapid in the presence of dATP. Also, the steady-state rate of dATP hydrolysis, after SSB protein displacement, is greater than that of rATP hydrolysis (32 versus 14 μM/min, respectively), suggesting that more SSB protein is displaced in the presence of dATP. Both of these results suggest that the dATP–recA protein complex can displace SSB protein from ssDNA more efficiently than the rATP–recA protein complex.

The physical explanation for this increased ability to displace SSB protein is unknown at this time. However, it is probably related to the dATP–recA protein complex having a higher steady-state affinity for ssDNA than the rATP complex (Menetski et al., 1988). This higher affinity for ssDNA may result in a dATP–recA protein complex which once bound to ssDNA would dissociate more slowly and prevent SSB protein from binding to the ssDNA. An alternative explanation is that the dATP–recA protein complex could occupy a vacant ssDNA site more rapidly than the rATP complex. Consistent with this hypothesis, the association rate of recA protein to ssDNA has been found to be 3–4 times faster in the presence of dATP than with rATP (Menetski, 1988). A final alternative is that the dATP–recA protein complex may actively displace SSB protein from ssDNA better than the rATP complex. Further studies will be required to discriminate between these possibilities. In any event, the presence of dATP appears to enhance the ability of recA protein to compete kinetically with SSB protein.

We have found that dATP can stimulate SSB displacement in the presence of excess rATP and that stimulation by dATP occurs at physiologically relevant concentrations of rATP and dATP (see Figure 3). The maximum apparent K_m values for dATP were found to be 160 and 400 μM dATP for the lag and rate data, respectively. The difference in the determined maximum K_m values is probably due to the fact that the rate

data are a composite of two effects: (1) the presence of dATP is probably increasing the amount of recA protein bound to M13 ssDNA, thus increasing the hydrolysis rate; and (2) dATP hydrolysis is faster than rATP hydrolysis, and the rate measured is of total nucleotide hydrolysis (ATP + dATP). These two effects make the analysis of the apparent K_m values determined from the rate data more difficult to interpret. The apparent K_m value determined from the lag data is more likely to reflect a simple relationship between the concentration of dATP and its effect on SSB displacement, since almost no hydrolysis occurs during the lag phase. Thus, if the in vivo concentration of rATP is 3 mM (Bochner & Ames, 1982), the apparent K_m for dATP in the SSB displacement reaction should be approximately 140 μM. This concentration is very close to the reported in vivo concentration of dATP (175 μM; Bochner & Ames, 1982).

The ability of recA protein to displace SSB protein from ssDNA in the presence of dATP may have important implications for in vivo recombination and SOS induction. Under cellular conditions, SSB protein may bind to ssDNA before recA protein. In the presence of rATP alone, this would greatly inhibit recA protein binding and, thus, SOS induction and recombination. By producing dATP, the cell may be able to increase the rate of recA protein binding to ssDNA by increasing the ability of recA protein to displace SSB protein from the ssDNA. Since the apparent K_m for this reaction is close to the in vivo concentration of dATP, small changes in the dATP concentration in vivo may have large effects on the rate of SSB protein displacement from ssDNA regions in the DNA. Roberts et al. (1982) have suggested that the cell may increase the concentration of dATP in response to DNA-damaging treatment by stimulating the enzyme ribonucleoside-diphosphate reductase. The activity of this enzyme is also stimulated when DNA replication is inhibited (Neuhard & Thomassen, 1971). Thus, even though there is a large excess of rATP in the cell (≈3 mM; Bochner & Ames, 1982), small changes in the concentration of dATP may make it an important cofactor for SOS induction and recombination.

A comparison of the NTP hydrolysis data and direct ssDNA binding data brings up a curious discrepancy. Saturation of NTP hydrolysis occurs at three nucleotides per recA protein monomer using either etheno M13 or poly(dT). A similar apparent site size has been observed for the DNA strand exchange reaction (two to four ssDNA nucleotides per recA protein monomer; Cox & Lehman, 1982), the coaggregation of ssDNA and dsDNA (two ssDNA nucleotides per recA protein monomer; Tsang et al., 1985), and λ repressor cleavage (three nucleotides per recA protein monomer; Craig & Roberts, 1981). However, direct recA protein binding studies, measuring the change in fluorescence of the etheno M13 DNA substrate (under conditions identical with those used in the rATPase activity assay), show that recA protein has an apparent site size of 7 (±1) nucleotides per recA protein monomer for both etheno M13 DNA (Menetski & Kowalczykowski, 1987a) and poly(dT).[2] The same stoichiometry is obtained whether protein is the titrant or etheno M13 DNA is the titrant (Kowalczykowski and Varghese, unpublished observations). Similarly, cross-linking of recA protein to poly(dT) shows an optimum at approximately seven nucleotides per recA protein monomer (Rehrauer and Kowalczykowski, unpublished observations). These results show that twice as much protein is required to saturate the NTP hydrolysis reaction than to saturate the ssDNA binding sites [for both etheno M13 DNA and poly(dT)]. A similar observation has been made by Mitchell et al. (1988). It is important to realize that the apparent discrepancy in observed stoichiometric requirements is due to the fact that the binding experiments measure a signal (i.e., fluorescence) that originates from the *ssDNA* whereas the NTPase experiments measures a signal (i.e., NTP hydrolysis) that originates from the *protein*. Thus, each is reporting a different aspect of complex formation.

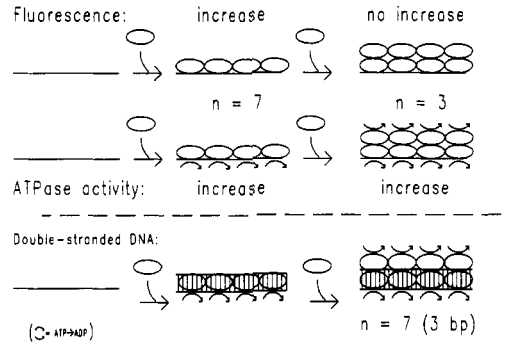

FIGURE 8: Model for recA protein binding to ssDNA and activation of rATP hydrolysis. Binding measurements utilize a signal originating from the DNA molecule; only direct contact with the DNA is reported. In contrast, rATPase activity reports the state of "activated" recA protein molecules. Thus, the data suggest that recA protein can directly interact with seven nucleotide residues but that an additional protein monomer can be activated to hydrolyze rATP by associating with a recA protein monomer within the protein–ssDNA filament. Expected binding and hydrolysis behavior is shown for both ssDNA and dsDNA. Apparent site size (n) is given in nucleotides per recA protein monomer. See the text for a detailed discussion of this model.

These data suggest a model for the recA protein–ssDNA complex which is shown in Figure 8. We assume that each recA protein monomer has an intrinsic ssDNA binding site size of six to seven nucleotide residues; this is consistent with the fluorescence binding data. However, NTPase activity is not saturated until another equivalent of recA protein binds to the recA protein–ssDNA complex (Figure 8, second row). This additional recA protein is activated for rATPase activity *without* binding to ssDNA, but rather by association with the first protein–ssDNA filament. This results in saturation of NTPase activity at 3–3.5 nucleotide residues per recA protein monomer. Thus, only one recA protein filament needs to bind to DNA to stimulate nucleotide hydrolysis by both recA protein filaments.[3] This model is further supported by results comparing the properties of the two recA protein filaments (Lauder and Kowalczykowski, unpublished observations). Pugh and Cox (1988) have reported that rATPase activity of recA protein can be activated at high salt concentrations in the absence of ssDNA. Thus, direct interaction with ssDNA is not always required to stimulate hydrolysis, and ssDNA may

[2] The apparent site size for poly(dT) can be determined from an etheno M13 DNA titration experiment, because the apparent affinity of recA protein for poly(dT) is greater than that for etheno M13 DNA. Adding recA protein to a mixture of poly(dT) and etheno M13 DNA results in binding to and saturation of the poly(dT) first (without changing the fluorescence of the etheno M13 DNA), followed by saturation of the etheno M13 DNA. This experiment yields identical apparent site sizes for etheno M13 and poly(dT) (Menetski and Kowalczykowski, unpublished observations).

[3] Other models for this phenomenon have been considered (e.g., monomer with two DNA binding sites). For the purposes of this paper, we wish to point out that different apparent site sizes are obtained experimentally and to propose one (of several) plausible model as a framework in which to view the apparently conflicting data. It is difficult to differentiate among these models with the data presented here; however, other results in the laboratory suggest that the dimeric filament model, as shown here, fits the data more completely (Lauder and Kowalczykowski, unpublished observations).

serve only as a scaffold to promote recA protein assembly at low salt concentrations. The assembly of a DNA-free protein filament onto a fiilament which is already bound to ssDNA may be sufficient to stimulate NTP hydrolysis of the second filament. It is not clear from these results whether recA protein exists as a dimer in solution. However, other data suggest that the dimeric filament may be produced only after DNA binding (Lauder and Kowalczykowski, unpublished observations).

This model can be used to further interpret the results of NTP hydrolysis experiments presented in this paper. The apparent site size of recA protein for poly(dA) determined by rATP hydrolysis is approximately six nucleotides per recA protein; this is twice the value obtained with either poly(dT) or etheno M13 DNA. However, in the presence of dATP, the apparent site size for poly(dA) decreases to three nucleotides per recA protein monomer with no change in k_{cat}. This result implies that in the presence of dATP, twice as much protein is associated with the poly(dA) but its hydrolytic capacity is unaltered. Since the affinity of recA protein for poly(dA) is lower than it is for either poly(dT) or etheno M13 DNA (McEntee et al., 1981a,b; Menetski & Kowalczykowski, 1985), it is possible that the ability of a DNA-bound monomeric filament to stimulate a second protein filament is linked to the affinity of recA protein for the ssDNA. If only recA protein molecules which are bound to ssDNA in a stable conformation can stimulate a "DNA-free" recA protein, the stability of the rATP–recA protein–poly(dA) complex may be too low to allow such stimulation. However, the more stable dATP–recA protein–poly(dA) complex can stimulate a recA protein which is not directly bound to ssDNA.

The results from the analysis of dsDNA-dependent NTP hydrolysis show that the apparent stoichiometry is 6 (±1) dsDNA nucleotide residues/recA protein. This result can also be interpreted by using the dimeric filament model as shown in Figure 8. In this case, the first monomeric filament can bind to one strand of the dsDNA, whereas the second is activated to associate either with the other DNA strand or with the first recA protein–DNA filament. Consequently, saturation of NTPase activity will occur at 6 base pairs (12 nucleotide residues) per 2 recA protein monomers, yielding an apparent site size of approximately 6 nucleotides/recA protein monomer (or 3 base pairs/monomer). Thus, this model for nucleotide hydrolysis can be used to interpret results from the analysis of both ssDNA and dsDNA. Further analysis of this phenomenon is likely to yield interesting results.

One of the most important implications of this model is that the active recA protein dimeric filament contains two DNA binding sites, one on each monomer. The ability to bind to two DNA molecules at the same time would explain several properties of recA protein. First, and most basic, is its ability to bind both a ssDNA molecule and a dsDNA molecule during the synaptic step of the DNA strand exchange reaction. Second, recA protein catalyzes renaturation of two complementary ssDNA molecules in a first-order reaction (McEntee, 1985); this observation is readily explained if recA protein were able to bind to both DNA molecules simultaneously. Third, the transfer of recA protein from one polynucleotide to another occurs through a ternary intermediate containing recA protein, the ssDNA molecule it was initially bound to, and the one to which it is transferring (Menetski & Kowalczykowski, 1987a,b). Further analysis must be carried out to determine the physical properties of the recA protein dimeric filament; however, it is clear that the ability of recA protein to bind to two DNA molecules simultaneously is essential during the DNA strand exchange reaction and in recombination in vivo. The involvement of a recA protein dimeric filament as a functional species provides a simple molecular solution for this requirement.

Acknowledgments

We thank Linda Roman, Angela Eggelston, Scott Lauder, Polly Lavery, Bill Rehrauer, and Dan Dixon for critically reviewing the manuscript. Also, we thank Dr. Stephen Brenner (E. I. du Pont de Nemours and Co.) for bringing the apparent site size discrepancy to our attention.

Registry No. dATP, 1927-31-7; rATP, 56-65-5; ATPase, 9000-83-3; dATPase, 51901-29-2.

References

Bochner, B. R., & Ames, B. N. (1982) *J. Biol. Chem. 257*, 9759–9769.

Bujalowski, W., & Lohman, T. M. (1986) *Biochemistry 25*, 7799–7802.

Chow, S. A., Rao, B. J., & Radding, C. M. (1988) *J. Biol. Chem. 263*, 200–209.

Cohen, S. P., Resnick, J., & Sussman, R. (1983) *J. Mol. Biol. 167*, 901–909.

Cox, M. M., & Lehman, I. R. (1981a) *Proc. Natl. Acad. Sci. U.S.A. 78*, 3433–3437.

Cox, M. M., & Lehman, I. R. (1981b) *Proc. Natl. Acad. Sci. U.S.A. 78*, 6018–6022.

Cox, M. M., & Lehman, I. R. (1982) *J. Biol. Chem. 257*, 8523–8532.

Craig, N. L., & Roberts, J. W. (1981) *J. Biol. Chem. 256*, 8039–8044.

Egelman, E. H., & Stasiak, A. (1986) *J. Mol. Biol. 191*, 677–697.

Griffith, J., & Shores, C. G. (1985) *Biochemistry 24*, 158–162.

Griffith, J. D., Harris, L. D., & Register, J., III (1984) *Cold Spring Harbor Symp. Quant. Biol. 49*, 553–559.

Kowalczykowski, S. C. (1986) *Biochemistry 25*, 5872–5881.

Kowalczykowski, S. C., & Krupp, R. A. (1987) *J. Mol. Biol. 193*, 97–113.

Kowalczykowski, S. C., Clow, J., & Krupp, R. A. (1987) *Proc. Natl. Acad. Sci. U.S.A. 84*, 3127–3131.

Kowalczykowski, S. C., Burk, D. L., & Krupp, R. A. (1989) *J. Mol. Biol. 207*, 719–733.

Lavery, P. E., & Kowalczykowski, S. C. (1988) *J. Mol. Biol. 203*, 861–874.

Lovett, C. M., Jr., & Roberts, J. W. (1985) *J. Biol. Chem. 260*, 3305–3313.

McEntee, K. (1985) *Biochemistry 24*, 4345–4351.

McEntee, K., Weinstock, G. M., & Lehman, I. R. (1981a) *J. Biol. Chem. 256*, 8835–8844.

McEntee, K., Weinstock, G. M., & Lehman, I. R. (1981b) *Prog. Nucleic Acid Res. Mol. Biol. 26*, 265–279.

Menetski, J. P. (1988) Ph.D. Thesis, Northwestern University.

Menetski, J. P., & Kowalczykowski, S. C. (1985) *J. Mol. Biol. 181*, 281–295.

Menetski, J. P., & Kowalczykowski, S. C. (1987a) *J. Biol. Chem. 262*, 2085–2092.

Menetski, J. P., & Kowalczykowski, S. C. (1987b) *J. Biol. Chem. 262*, 2093–2100.

Menetski, J. P., Varghese, A., & Kowalczykowski, S. C. (1988) *Biochemistry 27*, 1205–1212.

Messing, J. (1983) *Methods Enzymol. 101*, 20–78.

Michell, R. S., Zlotnick, A., & Brenner, S. L. (1988) *Biophys. J. 53*, 220a.

Morrical, S. W., Lee, J., & Cox, M. M. (1986) *Biochemistry 25*, 1482–1494.

Muniyappa, K., Shaner, S. L., Tsang, S. S., & Radding, C. M. (1984) *Proc. Natl. Acad. Sci. U.S.A. 81*, 2757–2761.
Neuhard, J., & Thomassen, E. (1971) *Eur. J. Biochem. 20*, 36–43.
Phizicky, E. M., & Roberts, J. W. (1981) *Cell 25*, 259–267.
Pugh, B. F., & Cox, M. M. (1987) *J. Biol. Chem. 262*, 1326–1336.
Pugh, B. F., & Cox, M. M. (1988) *J. Biol. Chem. 263*, 76–83.
Resnick, J., & Sussman, R. (1982) *Nucleic Acids Res. 10*, 5239–5253.
Roberts, J. W., Phizicky, E. M., Burbee, D. G., Roberts, C. W., & Moreau, P. L. (1982) *Biochimie 64*, 805–807.
Roman, L. J., & Kowalczykowski, S. C. (1986) *Biochemistry 25*, 7375–7385.
Schutte, B. C., & Cox, M. M. (1987) *Biochemistry 26*, 5616–5625.
Tsang, S. S., Chow, S. A., & Radding, C. M. (1985) *Biochemistry 24*, 3226–3232.
Tsang, S. S., Muniyappa, K., Azhderian, E., Gonda, D. K., Radding, C. M., Flory, J., & Chase, J. W. (1985) *J. Mol. Biol. 185*, 295–309.
Uhlin, B. E., & Clark, A. J. (1981) *J. Bacteriol. 148*, 386–390.
Uhlin, B. E., Schweikart, V., & Clark, A. J. (1983) *Gene 22*, 255–265.
Weinstock, G. M. (1982) *Biochimie 64*, 611–617.
Weinstock, G. M., McEntee, K., & Lehman, I. R. (1981) *J. Biol. Chem. 256*, 8829–8834.

Thermodynamic Comparison of the Base Pairs Formed by the Carcinogenic Lesion O^6-Methylguanine with Reference both to Watson–Crick Pairs and to Mismatched Pairs†

Barbara L. Gaffney and Roger A. Jones*
Department of Chemistry, Rutgers—The State University of New Jersey, Piscataway, New Jersey 08855
Received December 27, 1988; Revised Manuscript Received March 22, 1989

ABSTRACT: A set of 10 non-self-complementary nonadeoxyribonucleoside octaphosphates, d(GGTTXTTGG) and d(CCAAYAACC), where X and Y are A, C, G, T, or O⁶MeG, has been synthesized by a large-scale, automated, phosphoramidite procedure. Purification was effected by reversed-phase HPLC, and the base composition was verified by analytical HPLC after enzymatic degradation to the constituent deoxynucleosides. This set of molecules was designed to allow evaluation of the nearest-neighbor dependence of each base pair. The thermal stability, expressed as T_{max}, of each duplex containing one of the O⁶MeG base pairs, a Watson–Crick pair, or one of the mismatches possible with this set of molecules was determined over a concentration range of 5.7–200 μM. From these data the $\Delta H°$, $\Delta S°$, and $\Delta G°$ of each combination were calculated. In general, the relative thermal stabilities observed for the O^6-methylguanine combinations confirm our previous findings that the most stable base pair is formed with cytosine rather than thymine and that all O⁶MeG pairs are much weaker than Watson–Crick base pairs [Kuzmich, S., Marky, L. A., & Jones, R. A. (1983) *Nucleic Acids Res. 11*, 3393–3404; Gaffney, B. L., Marky, L. A., & Jones, R. A. (1984) *Biochemistry 23*, 5686–5691]. Moreover, the nine combinations containing O^6-methylguanine are all of similar thermal stability, cover a much smaller range in T_{max} than do the mismatches, and show little sequence dependence.

The generation of O^6-alkylguanine lesions in DNA has been implicated as an initiatory molecular event both to mutagenesis and to some types of carcinogenesis (Grunberger & Singer, 1983). For example, a single exposure of Buf/N rats to the methylating agent and carcinogen *N*-nitroso-*N*-methylurea (NMU) is sufficient to initiate malignancy and has been shown to produce a transforming Ha-ras-1 gene containing a specific G → A transition mutation (Zarbl et al., 1985). Moreover, low doses of the carcinogen 4-(*N*-methyl-*N*-nitrosoamino)-1-(3-pyridyl)-1-butanone (NNK), a major nitrosamine present in tobacco, which give rise to a high incidence of malignant lung tumors, also correlate with specific formation of O⁶MeG in lung Clara cells (Belinsky et al., 1987).

In human cell lines with low levels of the alkyltransferase required for repair of O⁶MeG, an increased sensitivity to the lethal and mutagenic effects of *N*-methyl-*N'*-nitrosoguanidine (MNNG) was observed (Domoradzki et al., 1984). Similarly, the leukemic transformation of rapidly proliferating bone marrow cells, induced by nitrosoureas, has been associated with their low levels of alkyltransferase (Gerson et al., 1987). Patients suffering from autoimmune diseases have also been found to be deficient in removal of O⁶MeG (Lawley, 1986).

It is known from experiments in which an oligonucleotide containing O⁶MeG was inserted into a viral or plasmid genome that O⁶MeG brings abount exclusively a G → A transition (Loechler et al., 1984; Chambers et al., 1985; Hill-Perkins et al., 1986; Bhanot et al., 1986; Topal et al., 1986). In addition, although the DNA sequence was shown to play a role in the *extent* of alkylation by NMU (Briscoe et al., 1985), the resulting mutations are always G → A (Richardson et al., 1987; Lucchesi et al., 1986). This strong preference for G → A transitions is consistent with the preferential pairing of O⁶MeG with thymine first postulated by Loveless (1969) and later supported on theoretical grounds (Klopman et al., 1982; Nagata et al., 1982). A later molecular mechanical simulation, however, concluded that there should be little or no difference in stability between O⁶MeG·C and O⁶MeG·T pairs (Caldwell & Kollman, 1985).

† This work was supported by NIH Grant GM 31483, American Cancer Society Grant CA 248B, an American Cancer Society Faculty Research Award to R.A.J., and the Busch Memorial Fund.

0006-2960/89/0428-5881$01.50/0